Design of Head Pursuit Guidance Law Based on Fractional-Order Sliding Mode Theory

Chenqi Zhu[1],*

1. Northwestern Polytechnical University – School of Cyberspace Security – Computer Science and Technology –Xi'an – China

*Corresponding author: 15036501865@163.com

This paper addresses problems on the interception of hypersonic vehicles in near-space. The main contribution is to study a head pursuit guidance law based on fractional-order sliding mode theory and analyze the stability of the guidance law provided. Firstly, the fractional-order differential operator, which has characteristics such as fast convergence and memory, is introduced into the design of sliding mode surface, based on which a head pursuit guidance can be designed to improve the performance of the guidance system. The stability of this guidance law is proved by Lyapunov stability theory. Based on this, a head pursuit guidance law considering autopilot dynamic characteristic is designed and the stability is also analyzed. Finally, numerical simulations are presented and the results verify that the guidance laws designed in this paper can avoid overload saturation at the initial moment of the terminal guidance stage and improve the convergence speed.

Keywords: Autopilot dynamic characteristic; Fractional-order sliding mode theory; Head pursuit guidance law; Near-space.

INTRODUCTION

With the development of near-space technology, hypersonic vehicles have been further amplified because of the characteristics such as fast flight speed, strong maneuvering ability, long flight distance and strong penetration ability. The traditional tail-chase interception requires the missile to be faster than the target, which will cause severe aerothermal ablation, affect the performance of the seeker and thus reduce the interception accuracy. Although traditional head-on interception can reduce the speed requirement of missile and avoid aerothermal ablation, it causes the relative speed to be so fast that the remaining flight time would be too short.

In order to solve the problems above, Golan and Shima (2004) provided a head pursuit guidance law for the first time. Based on this, Xiao *et al.* (2013) proposed an optimal adaptive sliding mode guidance (SMG) law to intercept hypersonic vehicle, which adopted the optimal sliding mode theory. For the purpose of attenuating chattering, Liu *et al.* (2015) introduced double-power reaching law and provided a head pursuit guidance law. Si and Song (2017) introduced a fast double-power reaching law into the design of head pursuit guidance law, which can improve the approach speed of sliding mode variables. Taking into account the uncertain dynamics of missile, Zhang *et al.* (2018) presented a head pursuit guidance law based on time-scale separation and varied the robustness to system disturbance. Zhu and Mu (2019) designed a head pursuit guidance law based on adaptive sliding mode control theory to intercept targets with high speed. But the overload saturation problem exists in all guidance laws above.

Compared with traditional sliding mode control theory, fractional-order sliding mode theory introduces fractional differential operator on the basis of traditional sliding mode, so it not only has the robustness of traditional sliding mode control but also has the memory and genetic characteristics of information, which can improve the performance of control system effectively. Therefore, fractional-order sliding mode theory has been widely studied in recent years. Pashaei and Badamchizadeh (2020) presented a fractional-order extended disturbance observer to estimate the matched and mismatched disturbances and their derivatives, based on which a fractional-order sliding mode controller was designed. Simulation results indicated that the controller had features of fast response, chattering reduction, robust stability and so on. Fei and Wang (2020) designed a fractional-order current harmonic compensation controller by combining the fractional-order sliding mode theory and recurrent neural network, which improved the performance of the active power filter. For the purpose of modeling the magneto rheological damper based on semiactive vehicle suspensions more precisely and making sure the finite time convergence of the system, Nguyen *et al.* (2020) proposed a fractional-order derivative based sliding mode controller and the validity of this controller is verified by numerical simulation. In order to enhance the output power quality of permanent magnet synchronous generator, Xiong *et al.* (2020) proposed a fractional-order sliding mode control (FOSMC) method, which decided the controller coefficient boundaries and had stronger robustness, superior tracking precision and faster time response. Rabah and Ladaci (2020) adopted adjustable parameters in the designing of sliding surface and proposed an adaptive fractional-order sliding mode controller to solve the synchronization problem for nonlinear fractional-order systems with chaotic behavior. Rahmani and Rahman (2020) proposed a fractional-order sliding mode controller to improve track tracking performance of 7 degrees of freedom (DOFs) exoskeleton robot named ETS-MARSE, which incorporated the adaptive radial basis function neural network with fast fractional integral terminal sliding mode control and addressed the chattering phenomena. In order to mitigate sub-synchronous control interaction, Li *et al.* (2020) proposed a fractional-order sliding mode controller which adopted genetic algorithm to optimize control parameters. Simulation results manifested that the controller had strong robustness and better damping performance. Sharafian *et al.* (2020) studied the HIV mathematical dynamic model and proposed a fractional-order observer to estimate the uncertainties, which was verified to have strong robustness. With the continuous improvement of fractional-order sliding mode theory, it has been applied to the field of aerospace gradually. Wang and Lei (2010) proposed a fractional-order guidance law based on the proportion integration differentiation (PID) guidance law, which improves the accuracy of interceptor and has strong robustness. In order to solve the problem of attitude tracking control for flexible spacecraft, fractional sliding mode controllers are proposed to make the systems have strong robustness and rapid convergence (Deng and Song 2013). Until now, fractional-order sliding mode theory has not been widely used in aerospace field. Therefore, this paper proposed head pursuit guidance laws based on fractional-order sliding mode theory for the interception of hypersonic vehicle.

The rest of this paper is organized as follows. In the upcoming section, some background information and preliminaries are introduced. Next, a head pursuit guidance law based on fractional-order sliding mode theory is designed and the stability is proved by Lyapunov stability theory. Furthermore, a fractional-order sliding mode head pursuit guidance law considering autopilot dynamic characteristics is designed and the stability is also analyzed. Finally, some numerical simulation comparisons in this study are summarized in the last part of the article.

METHODOLOGY

Problem formulation

Figure 1 depicts the schematic view of head pursuit interception between target and missile in longitudinal plane, where points T and M denote the target and the missile, r and q, the relative missile-target range and the line-of-sight (LOS) angle, θ_t and θ_m the lead angles, V_t and V_m velocities, a_t and a_m the components of accelerations perpendicular to the velocities, the subscripts t and m denote the target and missile.
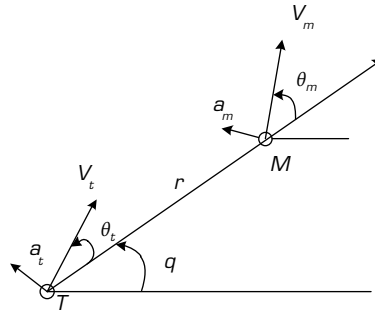
Figure 1. Relative motion schematic.

The respective equations describing the relative motion dynamics become:

$$\dot{r} = V_m \cos\theta_m - V_t \cos\theta_t \tag{1}$$

$$\dot{q} = (V_m \sin\theta_m - V_t \sin\theta_t)/r \tag{2}$$

$$\dot{\theta}_t = \frac{a_t}{V_t} - \dot{q} \tag{3}$$

$$\dot{\theta}_m = \frac{a_m}{V_m} - \dot{q} \tag{4}$$

Differentiating Eq. 2 with respect to time, it gets:

$$\ddot{q} = \frac{a_m \cos\theta_m}{r} - \frac{a_t \cos\theta_t}{r} - 2\frac{\dot{r}\dot{q}}{r} \tag{5}$$

According to the concept of head pursuit guidance law proposed by Golan and Shima (2004), if the lead angles θ_t and θ_m satisfy Eqs. 6 and 7, the target will be intercepted with zero miss-distance in the form of head pursuit interception:

$$\lim_{r \to 0}\theta_m = 0 \; ; \quad \lim_{r \to 0}\theta_t = 0 \tag{6}$$

$$\theta_m = n\theta_t \tag{7}$$

where n is a lead factor and satisfies $n > V_t/V_m$.

At the same time, it is proved that if the lead angles satisfied Eq. 7, the condition of Eq. 6 would be satisfied automatically (Golan and Shima 2004). Therefore, the purpose of the guidance law is to make the system satisfy Eq. 7. In the design of head pursuit guidance law, there are some assumptions as follows:

Assumption 1. The target and missile are point masses and the respective accelerations only change the direction of the velocity (Zhou *et al.* 2018).

Assumption 2. There is a minimum homing guidance distance r_0 so that the time-varying parameter $r(t)$ satisfies the following inequality (Zhou *et al.* 2018):

$$r(t) \geq r_0 \tag{8}$$

Assumption 3. The target and missile accelerations and their first derivatives are bounded (Zhou *et al.* 2018).

Assumption 4. According to the research presented by Golan and Shima (2004), the lead angles of target and missile satisfies the following constraints:

$$|\theta_t| < \sqrt{6\frac{Kn-1}{Kn^3-1}}; \quad |\theta_m| < n\sqrt{6\frac{Kn-1}{Kn^3-1}}$$

(9)

where K is a ratio and satisfies $K = V_t / V_m$.

Basic theories of fractional sliding mode

In the study of fractional-order theory, there are some definitions of fractional differential operators, such as Riemann-Liouville, Caputo and Grünwald–Letnikov definitions. In this paper, the Caputo definition is used.

Definition 1. The Caputo definition of continuous integrable function $f(t)$ is defined as follows (Dadras and Momeni 2012):

$$D^\alpha f(t) = \begin{cases} \dfrac{1}{\Gamma(m-a)} \displaystyle\int_0^t \dfrac{f^{(m)}(\tau)}{(t-\tau)^{a-m+1}} d\tau & (m-1 < \alpha < m) \\ \dfrac{d^m}{dt^m} f(t) & (\alpha = m) \end{cases}$$

(10)

where m is the smallest integer number which is larger than α, $\Gamma(\bullet)$ is the Gamma function. The notation D^α has different meanings for different values of α. When α is bigger than zero, D^α stands for fractional-order differentiation; when α is smaller than zero, D^α stands for fractional-order integral. Fractional differential operators D^α can be realized numerically by fractional-order toolbox (Tepljakov *et al.* 2011).

Similar to the integer order calculus, the fractional-order integration and differentiation (Dadras and Momeni 2012):

$$D^\alpha \left(D^\beta f(t) \right) = D^{\alpha+\beta} f(t) \quad (\alpha > 0)$$

(11)

$$D^0 f(t) = f(t)$$

(12)

When the fractional-order calculus operator is introduced into the sliding mode control law or sliding mode surface, it is called fractional-order sliding mode control. It not only has the robustness of traditional sliding mode control, but also has the memory and genetic properties of fractional-order differential operators, which can improve the performance of control system effectively.

Design of head pursuit guidance law based on fractional-order sliding mode theory

In this part, a head pursuit guidance law based on fractional-order sliding mode theory is designed for near-space hypersonic vehicle and the stability of the closed-loop system is analyzed.

Design of head pursuit guidance law

According to the discussion above, the error variable e is defined as follows:

$$e = \theta_m - n\theta_t$$

(13)

Differentiating Eq. 13 with respect to time and substituting Eqs. 3 and 4 into the result gives:

$$\dot{e} = \frac{a_m}{V_m} + (n-1)\dot{q} - \frac{na_t}{V_t}$$

(14)

The fractional-order sliding mode surface is defined as:

$$s_1 = k_1 e + D^\alpha e \tag{15}$$

where D^α is a fractional calculus operator and $k_1 \in \mathbf{R}^+$, $0 < \alpha < 1$.

Differentiating Eq. 15 with respect to time yields:

$$\dot{s}_1 = k_1 \dot{e} + D^{\alpha+1} e = \frac{k_1}{V_m} a_m + (n-1)k_1 \dot{q} + D^{\alpha+1} e - \frac{k_1 n}{V_t} a_t \tag{16}$$

According to assumption 3, the target acceleration satisfies $|a_t| \le \eta$, where $\eta \in \mathbf{R}^+$, then, a fractional-order sliding mode head pursuit guidance law can be designed as:

$$a_m = -V_m \left[\left(\frac{\varepsilon_1}{k_1} + \frac{n\eta}{V_t} \right) sign(s_1) + \frac{D^{\alpha+1} e}{k_1} + (n-1)\dot{q} \right] \tag{17}$$

where $\varepsilon_1 \in \mathbf{R}^+$.

Theorem 1. Consider Eqs. 1 to 4, the fractional-order sliding mode head pursuit guidance law, Eq. 17, will make the closed-loop system stable and the lead angles θ_t and θ_m will converge to zero.

Analysis of stability

In order to analyze the stability of the closed-loop system under the guidance law in Theorem 1, some lemmas are introduced here.

Lemma 1. Consider a nonlinear time-varying system as the form of $\dot{x} = f(x, t)$, $x \in R^n$, x is the system state and t is the time. If there is a continuous positive-definite function $V(x)$ which satisfies (Yu *et al.* 2005):

$$\dot{V}(x) + \mu V^\rho(x) \le 0 \tag{18}$$

where $\mu > 0$, $0 < \rho < 1$, the system state will converge to zero in finite-time T, which has the following form:

$$T \le \frac{1}{\mu(1-\rho)} V^{(1-\rho)}(x_0) \tag{19}$$

where $x(t_0) = x_0$, t_0 is the initial time.

Lemma 2. For the following fractional-order system (Aghababa 2013):

$$\begin{cases} D^\alpha x(t) = \mathbf{A}x(t) \\ x(0) = x_0 \end{cases} \tag{20}$$

where $x(t) \in \mathbf{R}^n$, $\mathbf{A} = [a_{ij}] \in \mathbf{R}^{m \times n}$, $0 < \alpha < 1$. If and only if the inequality (21) is true, the system (20) is asymptotically stable and the convergence rate of the system state is $t^{-\alpha}$:

$$\left| arg(\lambda_i(\mathbf{A})) \right| > \frac{\alpha}{2}\pi \tag{21}$$

Proof

Defining the following Lyapunov function candidate for Eq. 16:

$$V_1 = \frac{1}{2} s_1^2 \tag{22}$$

Computing time derivative of Eq. 22 along trajectories yields:

$$\dot{V}_1 = s_1 \dot{s}_1$$

$$= s_1 [- \varepsilon \, sign(s_1) - \frac{2}{V_t} \eta \, sign(s_1) - \frac{2}{V_t} a_t]$$

$$= - \varepsilon_1 |s_1| - \frac{2}{V_t} \eta |s_1| - \frac{2}{V_t} s_1 a_t$$

$$\leq - \varepsilon_1 |s_1| - \frac{2}{V_t} \eta |s_1| + \frac{2}{V_t} |s_1||a_t| \tag{23}$$

$$= - \varepsilon_1 |s_1| - \frac{2}{V_t} |s_1| (\eta - |a_t|)$$

$$\leq - \varepsilon_1 |s_1|$$

Which means that:

$$\dot{V}_1 + \sqrt{2} \varepsilon_1 V_1^{\frac{1}{2}} = \dot{V}_1 + \varepsilon_1 |s_1| \leq 0 \tag{24}$$

According to Lemma 1, the sliding variable S_1 will converge to zero in finite-time. So, the following equation can be given:

$$D^\alpha e = - k_1 e \tag{25}$$

According to Lemma 2, the error variable e converges to zero, therefore, the lead angles θ_t and θ_m will converge to zero.

Design of head pursuit guidance law considering the autopilot dynamic characteristic

Autopilot dynamic characteristic is also the main factor affecting interception accuracy, so it is necessary to consider it in the design of guidance law. Usually, the autopilot dynamic characteristic is approximated by the first-order inertia element as:

$$\dot{a}_m = - \frac{1}{\tau} a_m + \frac{1}{\tau} a_m^c \tag{26}$$

where a_m^c is acceleration instruction and τ is the time constant of dynamic delay.

Differentiating Eq. 14 with respect to time yields:

$$\ddot{e} = \frac{\dot{a}_m}{V_m} + (n - 1)\ddot{q} - \frac{n}{V_t} \dot{a}_t$$

$$= \frac{1}{V_m} \left[- \frac{1}{\tau} a_m + \frac{1}{\tau} a_m^c \right] + (n - 1)\ddot{q} - \frac{n}{V_t} \dot{a}_t \tag{27}$$

Substituting Eq. 5 into Eq. 27 gives Eq. 28:

$$\ddot{e} = \frac{1}{V_m} \left[- \frac{1}{\tau} a_m + \frac{1}{\tau} a_m^c \right] - \frac{n}{V_t} \dot{a}_t + (n - 1) \left(\frac{a_m \cos\theta_m}{r} - \frac{a_t \cos\theta_t}{r} - 2\frac{\dot{r}\dot{q}}{r} \right)$$

$$= \left[\frac{(n - 1)\cos\theta_m}{r} - \frac{1}{\tau V_m} \right] a_m - 2(n - 1)\frac{\dot{r}\dot{q}}{r} + \frac{1}{\tau V_m} a_m^c - \frac{(n - 1)\cos\theta_t}{r} a_t - \frac{n}{V_t} \dot{a}_t \tag{28}$$

Defining the intermediate variable y as:

$$y = k_2 e + \dot{e} \tag{29}$$

The fractional-order sliding mode surface is defined as follows:

$$s_2 = k_3 y + D^{\beta} y \tag{30}$$

where $k_3 \in R^+, 0 < \beta < 1$.

Differentiating Eq. 30 with respect to time yields:

$$
\begin{aligned}
\dot{s}_2 &= k_3 \dot{y} + D^{\beta+1} y \\
&= k_2 k_3 \dot{e} + k_3 \ddot{e} + D^{b+1} y \\
&= k_2 k_3 \left[\frac{a_m}{V_m} + (n-1)\dot{q} - \frac{n}{V_t} a_t \right] + k_3 \left\{ \frac{1}{V_m} \left[-\frac{1}{\tau} a_m + \frac{1}{\tau} a_m^c \right] + (n-1)\ddot{q} - \frac{n}{V_t} \dot{a}_t \right\} + D^{\beta+1} y \\
&= \frac{k_3}{V_m} \left(k_2 - \frac{1}{\tau} \right) a_m + k_2 k_3 (n-1)\dot{q} + D^{\beta+1} y + \frac{k_3}{V_m \tau} a_m^c + k_3 (n-1)\ddot{q} - \frac{n k_2 k_3}{V_t} a_t - k_3 \frac{n}{V_t} \dot{a}_t \\
&= \frac{k_3}{V_m} \left(k_2 - \frac{1}{\tau} \right) a_m + k_2 k_3 (n-1)\dot{q} + D^{\beta+1} y + \frac{k_3}{V_m \tau} a_m^c \\
&\quad + k_3 (n-1) \left(\frac{\cos\theta_m}{r} a_m - \frac{\cos\theta_t}{r} a_t - 2\frac{\dot{r}\dot{q}}{r} \right) - \frac{n k_2 k_3}{V_t} a_t - k_3 \frac{n}{V_t} \dot{a}_t \\
&= \left[\frac{1}{V_m} \left(k_2 - \frac{1}{\tau} \right) + (n-1)\frac{\cos\theta_m}{r} \right] k_3 a_m + \left(k_2 - 2k_3 \frac{\dot{r}}{r} \right)(n-1)\dot{q} \\
&\quad + D^{\beta+1} y + \frac{k_3}{V_m \tau} a_m^c + \left\{ -\left[(n-1)\frac{\cos\theta_t}{r} + \frac{n k_2}{V_t} \right] k_3 a_t - k_3 \frac{n}{V_t} \dot{a}_t \right\}
\end{aligned} \tag{31}
$$

The terms related to a_t in Eq. 31 are regarded as total disturbance d, in which n, k and V_t are positive constants. According to assumptions 2 to 4, r, θ_t, a_t and a_t are bounded, the following inequality can be:

$$
|d| = \left| -\left[(n-1)\frac{\cos\theta_t}{r} + \frac{n k_2}{V_t} \right] k_3 a_t - k_3 \frac{n}{V_t} \dot{a}_t \right| \leq k \tag{32}
$$

where $k \in R^+$. Therefore, Eq. 31 can be rewritten as:

$$
\dot{s}_2 = k_3 \left[\frac{1}{V_m} \left(k_2 - \frac{1}{\tau} \right) + (n-1)\frac{\cos\theta_m}{r} \right] a_m + \left(k_2 - 2k_3 \frac{\dot{r}}{r} \right)(n-1)\dot{q} + D^{b+1} y + \frac{k_3}{V_m \tau} a_m^c + d \tag{33}
$$

Designing the corresponding fractional-order sliding mode head pursuit guidance law as:

$$a_m^c = -\frac{V_m \tau}{k_3}\left\{\left[\frac{1}{V_m}\left(k_2 - \frac{1}{\tau}\right) + (n-1)\frac{\cos\theta_m}{r}\right]k_3 a_m + D^{\beta+1}y + \left(k_2 - 2k_3\frac{\dot{r}}{r}\right)(n-1)\dot{q} + (\varepsilon_2 + \kappa)sign(s_2)\right\} \quad (34)$$

where $\varepsilon_2 \in R^+$.

Theorem 2. Considering Eqs. 1-4 and the autopilot dynamic characteristic as Eq. 26, the head pursuit guidance law Eq. 34, based on fractional-order sliding mode theory, will make the closed-loop system stable and the lead angles θ_t and θ_m will converge to zero.

Proof

Define the Lyapunov function as:

$$V_2 = \frac{1}{2}s_2^2 \quad (35)$$

Computing time derivative of Eq. 35 along trajectories, it gets:

$$\begin{aligned}
\dot{V}_2 &= s_2\dot{s}_2 \\
&= s_2[-\varepsilon_2 sign(s_2) - k\,sign(s_2) + d] \\
&= -\varepsilon_2|s_2| - \kappa|s_2| + ds_2 \\
&\leq -\varepsilon_2|s_2| - \kappa|s_2| + |d||s_2| \\
&= -\varepsilon_2|s_2| - (\kappa - |d|)|s_2| \\
&\leq -\varepsilon_2|s_2|
\end{aligned} \quad (36)$$

Similar to Theorem 1, the sliding variable S_2 will converge to zero in finite-time and the following equation can be given:

$$D^\beta y = -k_3 y \quad (37)$$

According to Lemma 2, the intermediate variable y will converge to zero in finite time. Then, Eq. 29 can be rewritten as:

$$\dot{e} = -k_2 e \quad (38)$$

Obviously, error variable e is asymptotically stable. Therefore, the lead angles θ_t and θ_m will converge to zero.

RESULTS AND DISCUSSION

The effectiveness of the head-guidance laws based on fractional-order sliding mode theory proposed in this paper is evaluated by numerical simulation in this section.

The initial positions of the target and missile are set as (0m, 0m) and (4000 m, 5000 m), the initial velocities V_t=1600m/s and V_m=1200m/s, the initial lead angles $\theta_{t0} = -10°$, $\theta_{m0} = -15°$, the design parameter $n = 2$. The guidance laws are compared in two cases: target with constant maneuver and target with cosine maneuver.

The guidance law ignoring autopilot dynamic characteristic is rewritten as:

$$U_1 = a_m = - V_m \left[(\frac{\varepsilon_1}{k_1} + \frac{n\eta}{V_t})sign(s_1) + \frac{1}{k_1}D^{\alpha+1}e + (n-1)\dot{q} \right] \tag{39}$$

Set a = 1 and get the integer order guidance law as:

$$U_3 = - V_m \left[(\frac{\varepsilon_1}{k_1} + \frac{n\eta}{V_t})sign(s_1) + \ddot{e} + (n-1)\dot{q} \right] \tag{40}$$

The design parameters are $k_1 = 20$, $\varepsilon_1 = 0.5$, $\alpha = 0.13$ and $\eta = 50$.

When the target flies with $a_t = 49$ m/s^2, the simulation results of U_1 and U_3 are shown in Figs. 2 to 5.
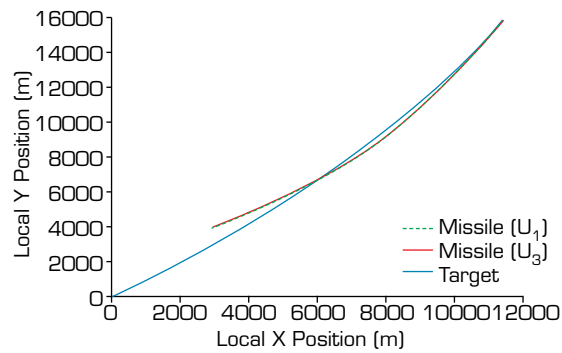
Figure 2. Relative motion orbit.
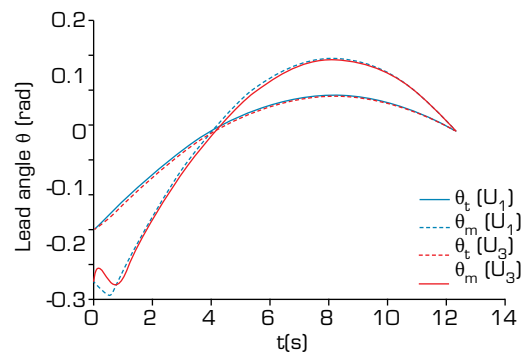
Figure 3. Lead angle θ.
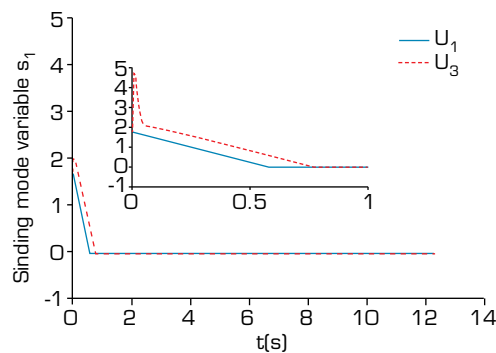
Figure 4. Sliding mode variable s_1.
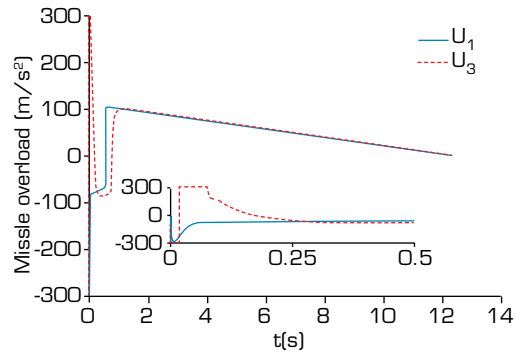
Figure 5. Missile overload a_m.

When the target flies with at = $49\cos(\pi t/4)$ m/s^2, the simulation results of U_2 and U_4 are shown in Figs. 6 to 9.
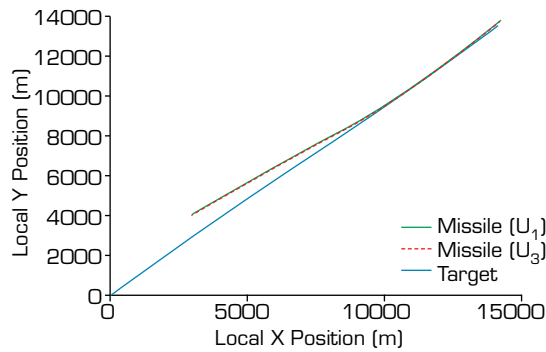
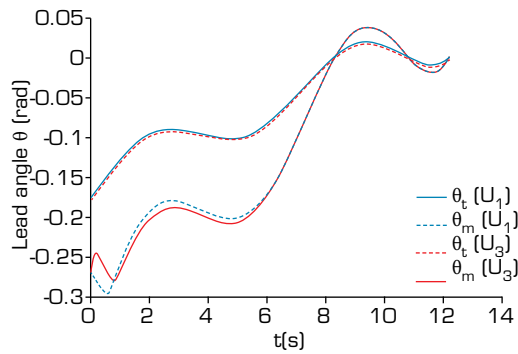**Figure 6.** Relative motion orbit.
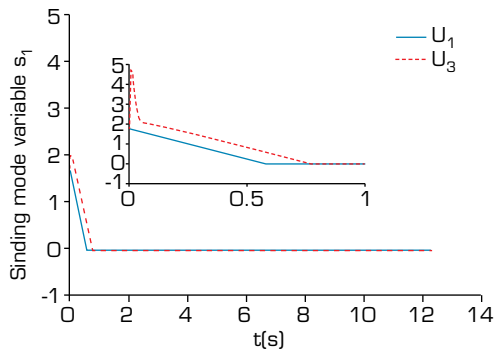

Figure 7. Lead angle θ.
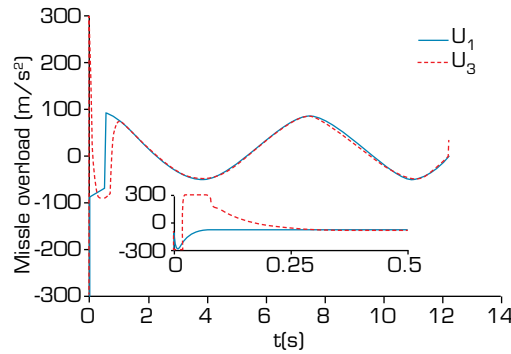

Figure 8. Sliding mode variable s_1.

Figure 9. Missile overload a_m.

Figures 2 and 6 show the relative motion orbits of the target and the missile, in both cases, the results indicate that both guidance laws can intercept the target in the form of head pursuit interception and have similar trajectories. Figures 3 and 7 show changing trend of lead angles, the results show that both guidance laws can adjust the leading angles to the states required in Eq. 7 and keep the state converging to zero. However, under the guidance law U_3, the leading angle of the interceptor will deviate from the state required in Eq. 7 temporarily. Figures 4 and 8 are the sliding mode variables, which show that the guidance law U_1 can make the sliding mode variables converge to zero faster. Figures 5 and 9 are the overloads required for head pursuit interception, which show that overload saturations occur at the initial stage of terminal guidance stage guided by U_3.

The miss distances of the two guidance laws are shown in Table 1, from which it can be seen that the miss distance under U_1 is better than that of U_3.

Table 1. Miss distances of U_1 and U_3.

Target acceleration	$\alpha = 0.13$	$\alpha = 1$
$a_t = 49$ m/s²	0.004	0.019
$a_t = 49 \cos(\pi t/4)$ m/s²	0.009	0.022

The guidance law considering the autopilot dynamic characteristic is rewritten as:

$$U_2 = a_m^c = - \frac{V_m \tau}{k_3} \left\{ \left[\frac{1}{V_m}\left(k_2 - \frac{1}{\tau} \right) + (n - 1)\frac{\cos\theta_m}{r} \right] k_3 a_m + \left(k_2 - 2k_3\frac{\dot{r}}{r} \right)(n - 1)\dot{q} + D^{\beta+1}y + (\varepsilon_2 + \kappa)sign(s_2) \right\} \quad (41)$$

Similarly, if $\beta = 1$, the integer order guidance law can be given as:

$$U_4 = - \frac{V_m \tau}{k_3} \left\{ \left[\frac{1}{V_m}\left(k_2 - \frac{1}{\tau} \right) + (n - 1)\frac{\cos\theta_m}{r} \right] k_3 a_m + \left(k_2 - 2k_3\frac{\dot{r}}{r} \right)(n - 1)\dot{q} + D^{\beta+1}y + (\varepsilon_2 + \kappa)sign(s_2) \right\} \quad (42)$$

The design parameter in U_2 and U_4 are $k_2 = 20$, $k_3 = 15$, $\varepsilon_2 = 0.5$, $\tau = 0.5$ $\beta = 0.13$ and $\kappa = 30$.

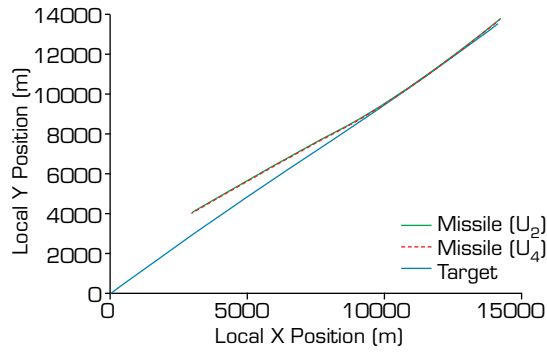When the target flies with at = 49 m/s², the simulation results of U_2 and U_4 are shown in Figs. 10 to 13.
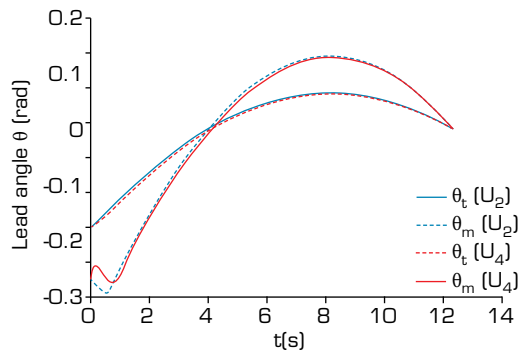
Figure 10. Relative motion orbit.
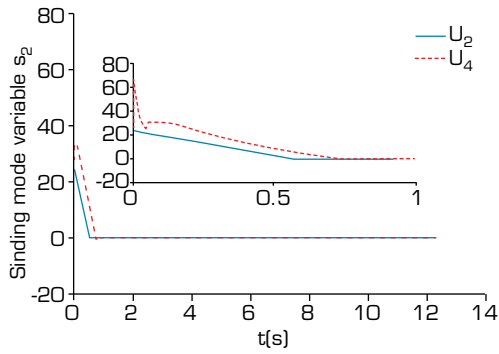

Figure 11. Lead angle θ.

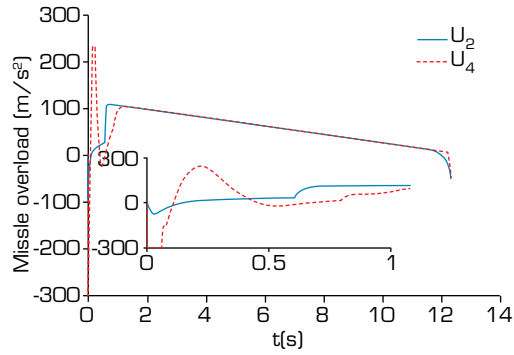**Figure 12.** Sliding mode variable s_2.

Figure 13. Missile overload a_m.

When the target flies with at $= 49 \cos(\pi t/4)$ m/s^2, the simulation results of U_2 and U_4 are shown in Figs. 14 to 17.
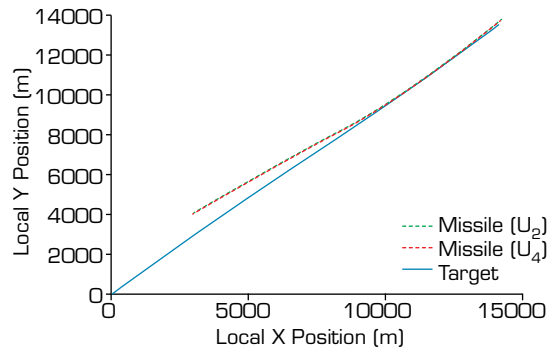

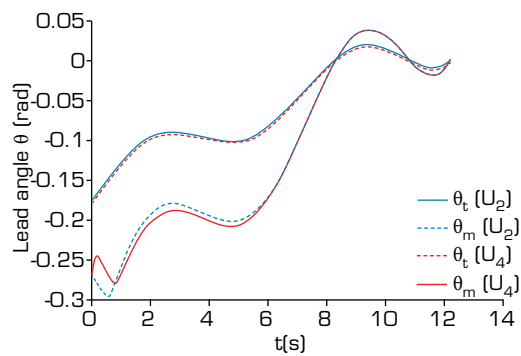**Figure 14.** Relative motion orbit.
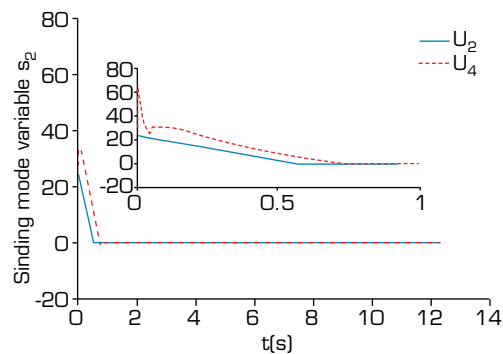

Figure 15. Lead angle θ.

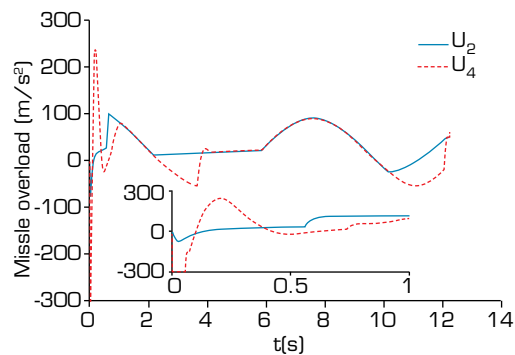**Figure 16.** Sliding mode variable s_2.

Figure 17. Missile overload a_m.

Figures 10 and 14 show that both guidance laws can achieve head pursuit interception under the consideration of autopilot dynamic characteristics. Figures 11 and 15 show the trends of the variables associated with lead angles, the results indicate that both guidance laws can make θ_m reach n times of θ_t in a very short time and the lead angles will converge to zero. But when the target is guided by U_4, the leading angle of the interceptor will deviate from the state required in Eq. 7 temporarily at the initial moment. Figures 12 and 16 are the sliding mode variables, which show that the sliding mode variables of both guidance laws can approach zero rapidly, but U_2 has a faster approach speed and without obvious chattering. Figures 13 and 17 are the overloads requirement of missile under two guidance laws. It is evident that the overload requirement of U_2 is lower than that of guidance law U_4 at the initial stage of terminal guidance stage.

The miss distances of the two guidance laws are shown in Table 2, from which it can be seen that the miss distance under U_2 is better than that of U_4.

Table 2. Miss distances of U_2 and U_4.

Target acceleration	$\alpha = 0.13$	$\alpha = 1$
$a_t = 49$ m/s^2	0.005	0.017
$a_t = 49 \cos(\pi t/4)$m/s^2	0.008	0.023

Remarks: The symbol function in the guidance law causes system chattering, so it is replaced by a saturation function as follows:

$$sat(s) = \begin{cases} 1 & s > \Delta \\ \dfrac{s}{\Delta} & |s| \leq \Delta \\ -1 & s < \Delta \end{cases} \tag{43}$$

where Δ is boundary layer thickness.

CONCLUSION

In order to intercept hypersonic vehicle in near-space, this paper proposes a head pursuit guidance law based on fractional-order sliding mode, which can not only avoid the problems of conventional guidance methods in intercepting hypersonic vehicle but also lower the requirements of missile velocity and overload capability and reduce miss distance. Besides, a head pursuit guidance law considering autopilot dynamic characteristic which can affect the interception accuracy is designed. Finally, numerical simulations verify the effectiveness of the guidance laws designed in this paper.

However, this paper only studies the interception of hypersonic vehicle by one interceptor, which may not guarantee a 100% interception rate. Furthermore, guidance law in this paper is only theoretical research and has not been verified in practice. Therefore, the next major focus of the research will be to study guidance law for multiple missiles against a hypersonic vehicle and verify the guidance law in this paper by practical application.

DATA AVAILABILITY STATEMENT

All the datasets were generated during the current study.

FUNDING

Not applicable.

ACKNOWLEDGEMENTS

REFERENCES

Aghababa MP (2013) A fractional-order controller for vibration suppression of uncertain structures. ISA Trans 52(6):881-887. https://doi.org/10.1016/j.isatra.2013.07.010

Deng L-W, Song S-M (2013) Robust Control of Spacecraft Attitude Based on Fractional Order Sliding-mode Controller. J Chinese Space Science and Technology. 33(4):1-8. https://doi.org/10.3780/j.issn.1000-758X.2013.04.001

Dadras S, Momeni HR (2012) Fractional terminal sliding mode control design for a class of dynamical systems with uncertainty. Commun Nonlinear Sci Numer Simul 17(1):367-377. https://doi.org/10.1016/j.cnsns.2011.04.032

Fei J, Wang H (2020) Recurrent neural network fractional-order sliding mode control of dynamic systems. J Franklin Inst 357(8):4574-4591. https://doi.org/10.1016/j.jfranklin.2020.01.050

Golan OM, Shima T (2004) Head Pursuit Guidance for Hypervelocity Interception. Paper presented AIAA Guidance, Navigation, and Control Conference and Exhibit. AIAA; Providence, Rhode Island. https://doi.org/10.2514/6.2004-4885

Liu K, Cao Y, Wang S, Li Y (2015) Terminal sliding mode control for landing on asteroids based on double power reaching law. Paper presented 2015 IEEE International Conference on Information and Automation. IEEE; Lijiang, China. https://doi.org/10.1109/ICInfA.2015.7279696

Li P, Wang J, Xiong L, Ma M, Wang Z, Huang S (2020) Mitigating subsynchronous control interaction using fractional sliding mode control of wind farm. J Franklin Inst 357(14):9523-9542. https://doi.org/10.1016/j.jfranklin.2020.07.024

Nguyen SD, Lam BD, Ngo VH (2020) Fractional-order sliding-mode controller for semi-active vehicle MRD suspensions. Nonlinear Dyn 101(2):795-821. Doi: 10.1007/s11071-020-05818-w.

Pashaei S, Badamchizadeh MA (2020) Control of a class of fractional-order systems with mismatched disturbances via fractional-order sliding mode controller. Trans Inst Meas Control 42(13):2423-2439. https://doi.org/10.1177/0142331220912070

Rabah K, Ladaci S (2020) A Fractional Adaptive Sliding Mode Control Configuration for Synchronizing Disturbed Fractional-Order Chaotic Systems. Circuits Syst Signal Process 39(3):1244-1264. https://doi.org/10.1007/s00034-019-01205-y

Rahmani M, Rahman MH (2020) Adaptive Neural Network Fast Fractional Sliding Mode Control of a 7-DOF Exoskeleton Robot. Int J Control Autom Syst 18(7):124-133. https://doi.org/10.1007/s12555-019-0155-1

Sharafian A, Sharifi A, Zhang W (2020) Fractional sliding mode based on RBF neural network observer: Application to HIV infection mathematical model. Comput Math with Appl 79(11):3179-3188. https://doi.org/10.1016/j.camwa.2020.01.014

Si Y, Song SM (2017) Adaptive reaching law based three-dimensional finite-time guidance law against maneuvering targets with input saturation. Aerosp Sci Technol 70:198-210. https://doi.org/10.1016/j.ast.2017.08.006

Tepljakov A, Petlenkov E, Belikov J (2011) Fomcon: Fractional-Order Modeling and Control Toolbox for Matlab. Paper presented 18th International Conference-Mixed Design of Integrated Circuits and Systems. IEEE; Gliwice, Poland.

Wang F, Lei H-M (2010) PDλ guidance law based on fractional calculus. Control Theory & Applications 27(1):126-130.

Xiao K, Sun B, Zhang W, Cai Y (2013) Head Pursuit Optimal Adaptive Sliding Mode Guidance Law. J IFAC Proceedings Volumes 46(13):508-513. https://doi.org/10.3182/20130708-3-CN-2036.00096

Xiong L, Li P, Ma M, Wang Z, Wang J (2020) Output power quality enhancement of PMSG with fractional order sliding mode control. Int J Electr Power Energy Syst 115:105402. https://doi.org/10.1016/j.ijepes.2019.105402

Yu S, Yu X, Shirinzadeh B, Man Z (2005) Continuous finite-time control for robotic manipulators with terminal sliding mode. Automatica 41(11):1957-1964. https://doi.org/10.1016/j.automatica.2005.07.001

Zhang Y, Wu H, Liu J, Sun Y (2018) A blended control strategy for intercepting high-speed target in high altitude. Proc IMechE Part G: J Aerospace Engineering 323(12):2263-2285. https://doi.org/10.1177/0954410017718569

Zhou H-B, Song J-H, Song S-M (2018) Sliding Mode Guidance Law Considering Missile Dynamic Characteristics and Impact Angle Constraints. J International Journal of Automation and Computing 15(2):218-227. https://doi.org/10.1007/s11633-016-0953-y

Zhu C, Mu D (2019) Design of head-pursuit guidance law based on sliding mode control. IOP Conf Ser: Mater Sci Eng 563(4):042076 https://doi.org/10.1088/1757-899X/563/4/042076